ELSEVIER

Ceramics International 30 (2004) 177–183

CERAMICS INTERNATIONAL

www.elsevier.com/locate/ceramint

# Finite element simulation of cold isostatic pressing and sintering of SiC components

M. Reiterer[a,*,1], T. Kraft[a], U. Janosovits[b], H. Riedel[a]

[a]*Fraunhofer-Institute for Mechanics of Materials, Wöhlerstrasse 11, 79108 Freiburg, Germany*
[b]*H.C. Starck Ceramics GmbH & Co. KG, Lorenz-Hutschenreuther-Str. 81, 95100 Selb, Germany*

Received 11 February 2003; received in revised form 3 March 2003; accepted 4 April 2003

**Abstract**

Finite element simulations were performed for cold isostatic pressing of SiC powder. To describe the compaction behaviour, the Drucker–Prager–Cap model implemented in ABAQUS/Explicit® computer program was applied. The influence of friction between powder and steel core as well as rubber bag on the density distribution was investigated for compacts with cylindrical and helical cores. Simulations with and without rubber bags were made showing that the effect of the bag on the density distribution is fairly small, at least for thin bags. Due to the presence of the steel core, density gradients develop during compaction, although the outer pressure is hydrostatic. The predicted density variation is consistent with experimental results. After the pressing cycle it may be difficult to remove the helical steel core from the powder compact. The simulation shows that the elastic spring-back leads to residual stresses which may reach the green strength of the powder compact, so that the part may crack during the unloading or removal of the helical core. Investigations of the sintering behaviour predict small shape distortions due to the slightly inhomogeneous density distribution of the green body. However, the differences between the ideal geometry and the predicted outline after sintering are small.


*Keywords:* A. Pressing; A. Sintering; D. SiC; Simulation

## 1. Introduction

Cold isostatic pressing (CIP) is a shaping technique in powder technology which is frequently used for the production of relatively large parts. The powder is filled into a rubber bag having the desired shape. If tube-like parts are to be made, a steel core is mounted in the rubber bag. In the so called wet-bag process the whole rubber bag containing the powder and the core is immersed in oil, which is then pressurized. In the absence of a core, the pressure and the resulting density are homogeneous in the powder compact (apart from small disturbances due to the small rigidity of the thin-walled rubber bag). The presence of a steel core leads to an inhomogeneous density distribution, but compared to density gradients after die compaction, the density is still rather homogeneous after cold isostatic pressing. Hence, the sinter distortions are relatively small. On the other hand, a green body formed by a soft rubber bag does not have as good a geometrical surface accuracy as does a die-pressed part. Therefore, cold isostatically pressed parts are usually machined in the green state.

In the present paper cold isostatic pressing is analyzed numerically using the finite element method together with an appropriate constitutive model for powder. The simulation helps to understand the roles of the core, of the friction between the core and the powder, and of the rubber bag on the density distribution. It also addresses the question under which conditions helical cores can be removed from the powder compact. A better understanding and a detailed simulation of the process leads to reduced cost and time for the development of new parts.

Compared to die compaction, modelling of cold isostatic pressing has been studied and published less

* Corresponding author. Tel.: +49-761-5142-235; fax: +49-761-5142-110.
*E-mail address:* reit@iwm.fhg.de (M. Reiterer).
[1] On leave from: Department of Structural and Functional Ceramics University of Leoben, Peter-Tunner-Strasse 5, 8700 Leoben, Austria.

0272-8842/03/$30.00 
doi:10.1016/S0272-8842(03)00086-5

frequently. However, the constitutive equations and the systematics in modelling are similar. A summary of the state of the art in simulating die compaction is given in [1–3]. A recent compilation of modelling activities concerning powder compaction is presented in [4]. Henderson et al. [5] have used a constitutive law with an elliptic yield surface [6] for the powder and a hyperelastic model for the rubber mould in their investigations of CIP. They predict green shapes accurately and conclude that the influence of the rubber bag increases with its thickness, and cannot be neglected for complex three-dimensional parts. The consolidation behaviour of SiC powder during triaxial compression was investigated by Park and Kim [7], who compared three different materials models by using FEM and found reasonable agreement with the experiments for all of these. Both Henderson et al. [5] and Park and Kim [7] performed the simulations with ABAQUS/Standard®.

## 2. Constitutive model

Continuum plasticity models are frequently used to describe the mechanical response of powders during compaction. These phenomenological models, which were originally developed in soil mechanics, are characterised by a yield criterion, a hardening function and a flow rule. The present work is based on the Drucker–Prager–Cap model. The yield surface of this model consists of an elliptic cap [8] and a straight failure line [9] in the plane of first and second stress invariant. Inside the yield surface, the powder behaves elastically. If the stress state reaches the yield surface, the powder deforms plastically. In the case of CIP the stress state is close to the axis of the first invariant, which is the pressure. Moderate deviations from the isostatic stress state occur near the steel core or near the corner of the rubber bag.

In contrast to the authors mentioned above, we use a dynamic explicit code for compaction simulations, which has several advantages compared to implicit codes, e.g., the possibility of large element distortions or computationally faster implementations of contact algorithms. This will be favourable for simulating the contact between the core or the rubber bag and the powder. We employed the Modified Drucker–Prager–Cap model, which is offered besides other soil mechanics material models in the ABAQUS/Explicit® computer program [10]. In ABAQUS the hardening variable $p_b$ is a variable depending on the volumetric strain (which is equivalent to density), whereas the cap eccentricity parameter $R$, the cohesion strength $d$, and the cohesion angle $\beta$ are constants. (For the definition of $p_b$, $d$ and $\beta$, see Fig. 1.) Using constant values for $R$, $d$ and $\beta$ seems to be a sufficient assumption, since the variations are often very small in ceramic powders as for example for SiC [11].

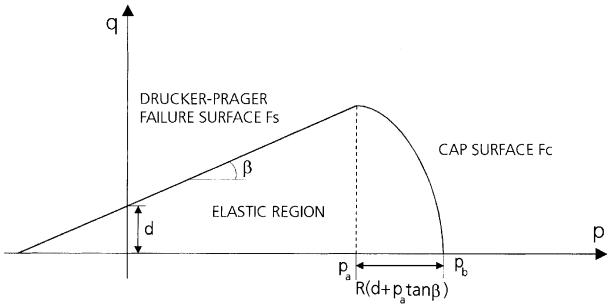


Fig. 1. Drucker–Prager–Cap model in the $p$–$q$ plane ($p$ = hydrostatic pressure, $q$ = Mises stress).

However, for describing the hardening behaviour of the powder, the density dependence must be considered. The volumetric strain is related to the density by

$$\varepsilon_{\mathrm{vol}}^{P} = \ln\left(\frac{\rho}{\rho_0}\right)$$

with the fill density $\rho_0$ and the actual density $\rho$. The hardening of the powder is taken from die pressing tests (see below) and entered in tabular form to the input deck.

## 3. Material and experiments

The work was carried out with a SiC powder, which was provided by H.C. Starck, Selb, Germany. Uniaxial die pressing experiments were conducted to determine the required parameters for the FE simulation. Fig. 2 shows measured densification curves of several experiments up to a pressure of 225 MPa. A friction coefficient $\mu_s$ of 0.22 between powder and steel core was measured using the method of Strijbos [12]. For the contact between powder and rubber bag $\mu_r = 0.4$ was assumed.

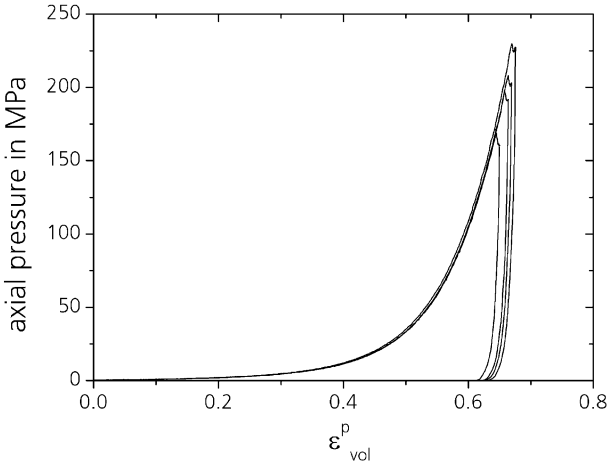


Fig. 2. Densification behaviour for the SiC powder.

## 4. Simulation of cold isostatic compaction

### 4.1. Compaction of axisymmetric parts

Hollow cylinders, which are pressed on a steel core, were investigated first in this work. Applying a hydrostatic pressure of 180 MPa and its release were simulated for all examples shown below. If not mentioned explicitly, the pressure was applied directly to the powder surface in the simulation, which means that the rubber bag was omitted. This simplification is justified later.

Figs. 3 and 4 show an example of a simulation. The diameters of the core and the rubber bag were 55 mm and 125 mm, respectively, and the initial height was 398 mm. The symmetry of the problem allows to model only the upper half of the axisymmetric part. Fig. 3 shows the finite element mesh of the loose powder and the pressed green body. The plastic volumetric strain of the green body after compaction is shown in Fig. 4. It is interesting to note that even without a rubber bag so-called "elephant feet" develop at the top of the specimen in Figs. 3 and 4. Fig. 5 shows the distribution of the stress components, of the von Mises equivalent stress and of the pressure.

Both experiment and simulation show a maximum density near the core. The decrease from the core to the outer edge is expected due to the conditions of stress equilibrium. The stress state of the powder directly at the core is different from a pure hydrostatic stress state in that the material cannot move inwards with increasing compaction. This leads to compressive stresses in the circumferential direction (Fig. 5) and, thus, to the observed maximum in density. For core/rubber bag diameters of 50/200 mm a detailed study was performed to determine the influence of the friction coefficient $\mu_s$ on the density distribution. Fig. 6 shows the calculated density variation along the radius in the middle plane of the cylinder, i.e., along the horizontal line at the bottom of Figs. 3–5. The results of the simulation with various friction coefficients are compared with the experimental density distribution. Although there is a difference in the absolute values of the measured and calculated densities, the tendency is the same for a realistic friction coefficient of $\mu_s = 0.25$ (Fig. 6). The reason for the difference in absolute values might be that the experiment was performed some years ago with a SiC powder possibly somewhat different from the powder used in this study.

The slight increase of the density towards the outer edge is more difficult to understand. Apparently it depends on the details of the yield surface of the Drucker–Prager–Cap model in combination with the friction effects at the core in axial direction. Without friction or with steel end caps (top-covers) this slight increase towards the outer edge is not predicted. Therefore, a possible qualitative explanation would be that friction lowers the density level and this effect decays

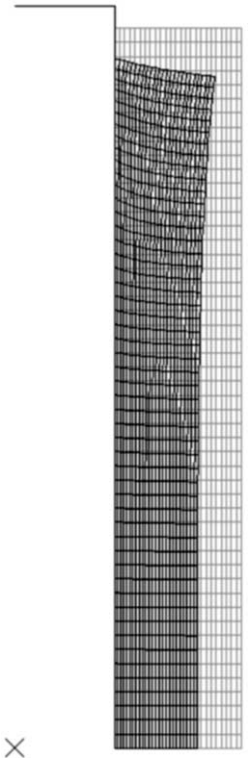

Fig. 3. FE mesh of the loose powder and after compaction for the reference case ($\mu_s = 0.22$, $\mu_r = 0.4$).

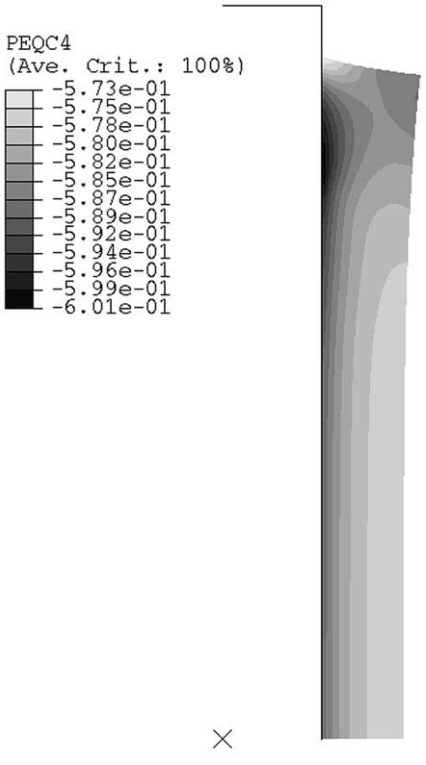


Fig. 4. Plastic volumetric strain of the green body without rubber bag.

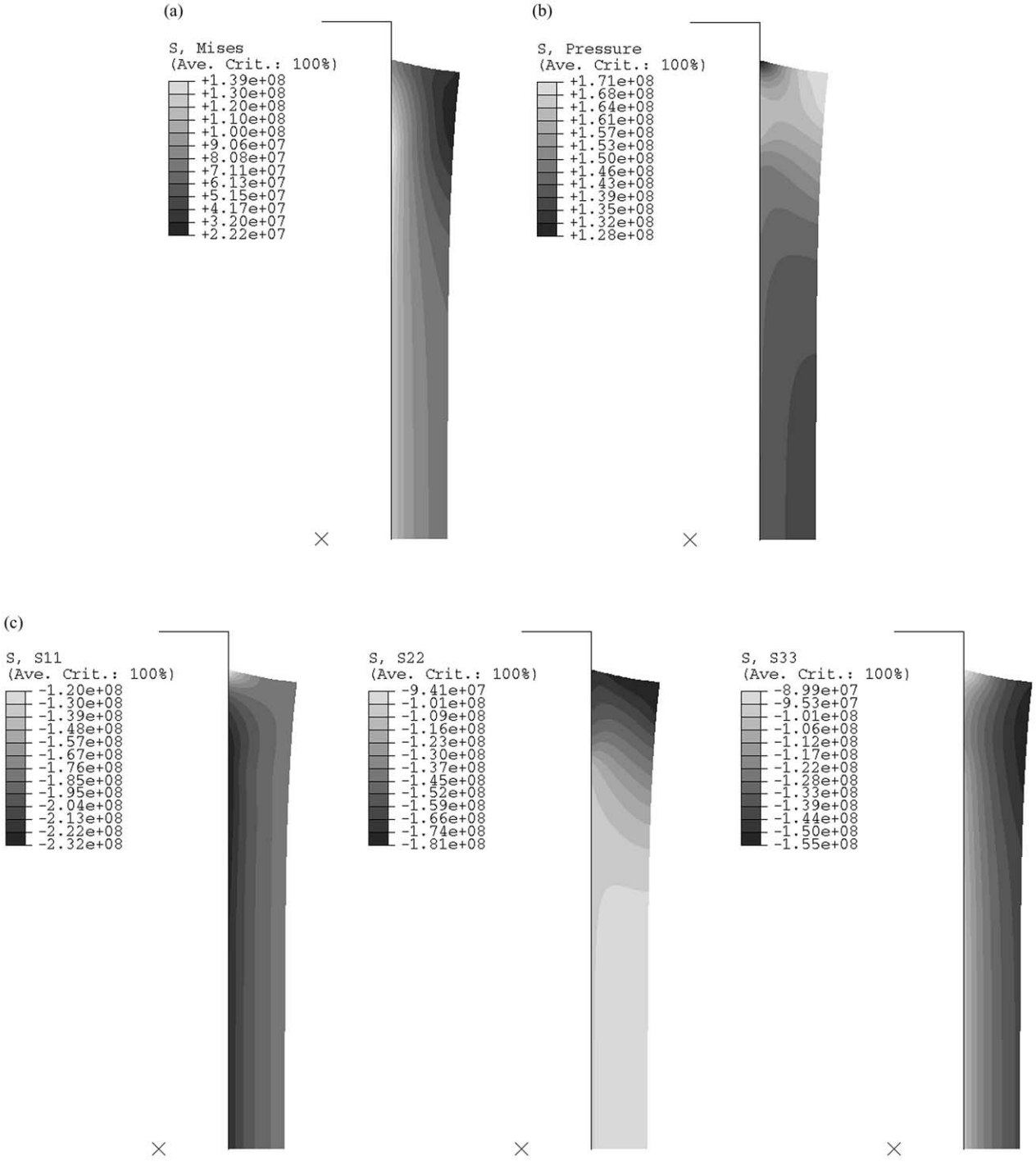


Fig. 5. von Mises (a) and hydrostatic (b) stress as well as the stresses in the single directions (c) of the green body at a pressure of 180 MPa for $\mu_s = 0.22$.

further away from the core, so that the density can increase towards the edge.

### 4.2. Compaction of an axisymmetric part under the influence of the rubber bag

In this section, the influence of the rubber bag is investigated numerically by means of a cylinder with a bag diameter of 125 mm and a bag thickness of 2 mm. In practice, bags with larger wall thickness are used. Incompressible or nearly incompressible materials such as rubber are often difficult to simulate with explicit finite element (FE) codes [10]. However, the numerical difficulties have been solved by selecting a hyperelastic material model implemented in ABAQUS® and using proper material parameters. A partial section of the FE

mesh before and after compaction is shown in Fig. 7. The density distribution in the green body differs only slightly between simulations with and without rubber bag, see Figs. 8 and 4, respectively. Both figures show the compact after densification to 180 MPa at a remaining pressure of 18 MPa. Lowering the pressure further leads to numerical problems; the rubber bag then expands dynamically, a problem which can occur in a dynamic explicit code, and which could be resolved if needed. However, since the shape and density distribution of the green body are not influenced by this small remaining pressure, the simulation was determined at 18 MPa. In Table 1 the compacted dimensions of the experiment and the calculations are presented. The simulation gives somewhat larger "elephant feet" and heights than the experiment, but this seems to be within the experimental inaccuracy. These results indicate that the agreement with experimental data is sufficient for practical purposes and that the bag can be omitted in the simulations, at least for thin bags.

Other authors have also investigated the influence of the bag for simple geometries. Kim et al. [13] investigated the effect of a rubber bag on densification behaviour. Similar to our observation they found a good general agreement with the experimental data, with small deviations of the predicted shape at the very corner. Henderson et al. [5] reported that the influence of

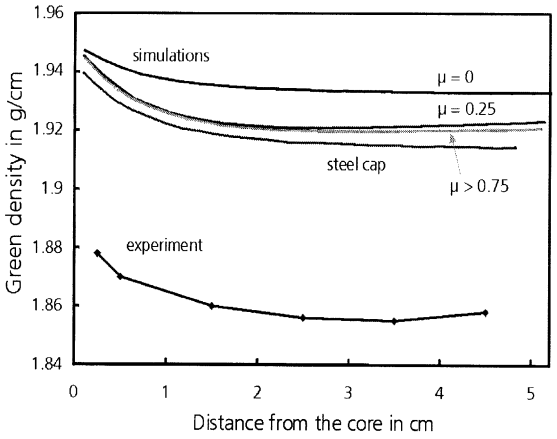


Fig. 6. Comparison of the green density of an experiment and several simulations (variation of $\mu_s$ or with a steel cap at the end).

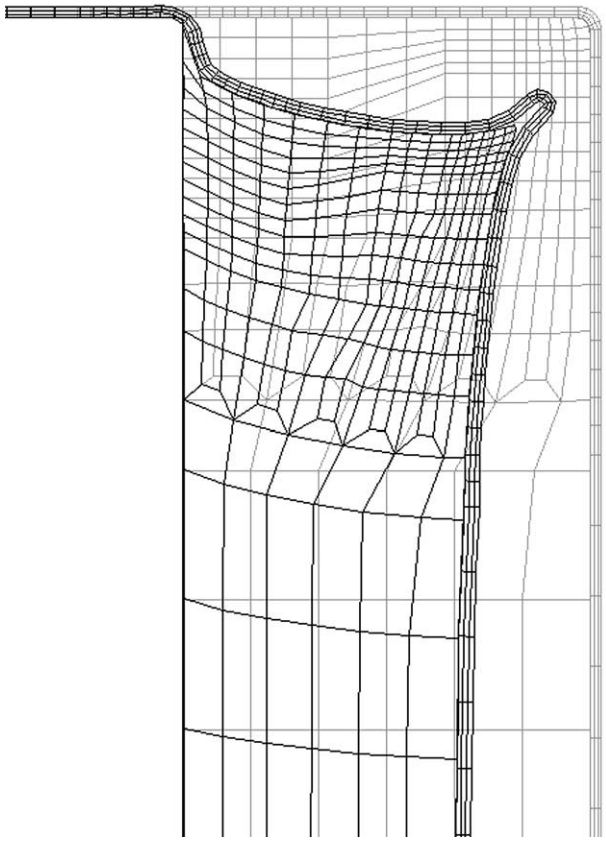

Fig. 7. Corner region of the FE mesh before and after pressing. An outer pressure of 18 MPa is still present, which does not change the results for the compact.

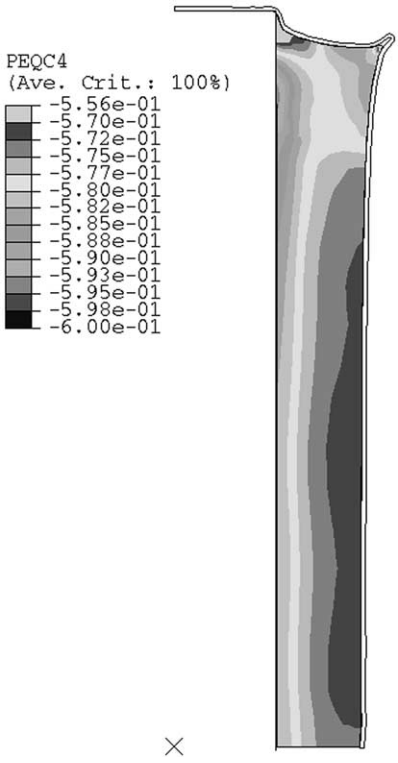


Fig. 8. Density distribution of the green body.

Table 1
Dimensions of the green bodies

| | Overall length | Max. diameter (at the top) | Min. diameter (at the middle) |
|---|---|---|---|
| Experiment | 368 | 106 | 102 |
| Simulation without rubber bag | 371 | 110 | 101 |
| Simulation with rubber bag | 376 | 112 | 101 |

the rubber is only significant at the early stages of pressing, as long as the stiffness of the bag is higher than the stiffness of the powder. Hence, thicker bags have a greater effect on the compaction behaviour.

## 5. Simulation of compaction and sintering of a feeder screw

Finally, cold isostatic pressing of a feeder screw was studied considering also the sintering process following afterwards. A pressure of 180 MPa was applied directly on the powder surface. Spring back was considered as well. Fig. 9a shows the FE mesh of the loose powder prior to consolidation. In Fig. 9b, the mesh of the released green body is displayed where the influence of the friction ($\mu_s = 0.22$) on the helical steel mandrel is visible. The steel mandrel itself is shown in Fig. 9c.

Fig. 10 demonstrates that a fairly homogeneous density distribution of the compact is predicted. Some slight differences develop with the region of highest density being located at the mandrel. It was observed experimentally that the green body is difficult to remove from the mandrel.

This is confirmed by the numerical results, which predict contact pressures up to 1.6 MPa (Fig. 11) after releasing the outer pressure. A green strength of about 1 MPa is typically measured for SiC powder compacts pressed with 180 MPa. The FE simulations show that the residual stresses are in the same order of magnitude as the green strength and, therefore, predict the reason for failure. If the green strength would rise superproportionally to compaction pressure, the problem

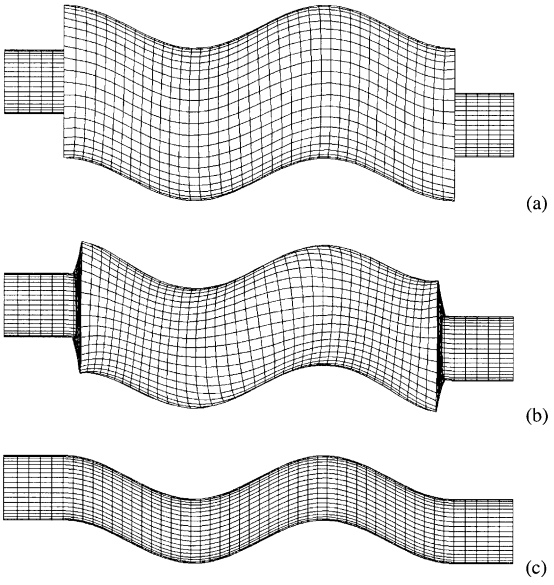


Fig. 9. FE mesh of the loose powder (initial stage)/(a), the green body (final stage)/(b) and the helical mandrel (c).

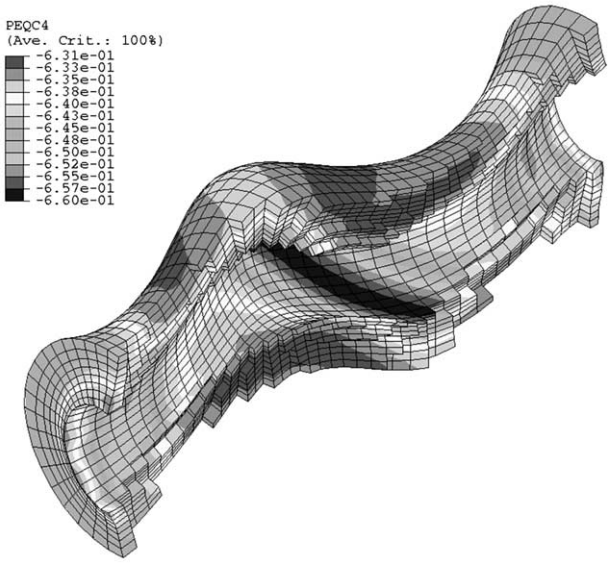


Fig. 10. Density distribution of the green body after pressure release.

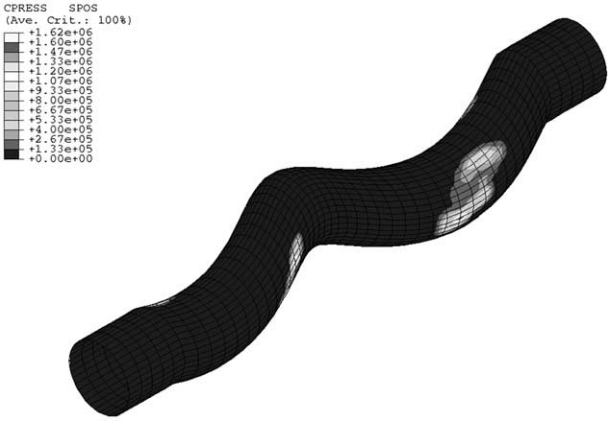


Fig. 11. Contact pressure on the mandrel after pressure release.

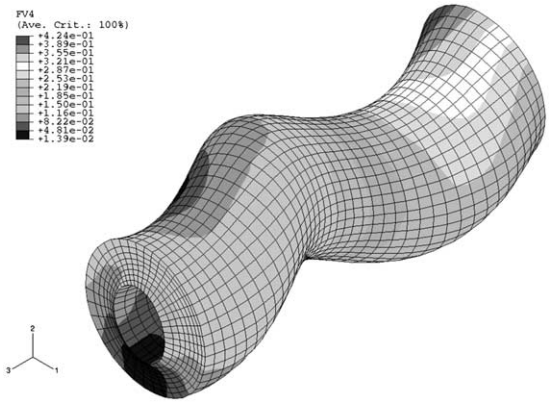


Fig. 12. Deviations in the sintering contour between simulations with homogeneous and with calculated initial density distributions. Differences of the nodal coordinates after sintering are shown in mm.

could be solved by applying a higher pressure. However, this has not been investigated up to now.

In order to reduce difficult machining, minimum shape distortion is a key feature for all kinds of powder technological components [14]. Sintering behaviour and warpage can be predicted by the use of FE in combination with a suitable material model. Here, a micromechanical model for solid state sintering [15] was applied, which is implemented as a user subroutine in ABAQUS/Explicit®. For a face seal made from SiC, the procedure is described in detail by Kraft and Riedel [15]. The material parameters for SiC needed for the sintering simulation are also taken from this paper.

For the evaluation of warpage two cases were considered: Firstly, the sintering of a green body with an ideal homogenous green density and the average value from the compaction simulation was calculated in order to get the ideal shape of the component. Secondly, the same simulation was conducted with the previously calculated density distribution. The deviations between both cases are shown in Fig. 12 by subtracting the nodal coordinates of both results (Fig. 12). The maximal difference was 0.4 mm.

## 6. Summary and concluding remarks

In the present work, the capabilities of finite element simulations for cold isostatic pressing are investigated, using the Drucker–Prager–Cap model as implemented in ABAQUS/Explicit®. Friction and uniaxial die pressing tests were performed to determine the friction coefficient and the material parameters of a commercial SiC powder.

Two part geometries were considered. First, CIPping of hollow cylinders was simulated and experimentally validated. An inhomogeneous density distribution is observed despite the presence of a hydrostatic pressure applied at the outline. The gradient results directly from the details of the yield surface of the Drucker–Prager–Cap model in combination with the powder interaction with the core rod. By comparing two simulations of the same geometry, one with and one without rubber bag, it was found that omitting the bag influences the density distribution only slightly at least for thin bags. "Elephant feet" occur even if the rubber bag is omitted from the simulation. Their magnitude is slightly enhanced by the rubber bag. The influence of the rubber bag increases with its thickness and may be important for more complex parts, if there are bulky moulds applied.

In the second part, CIPing and sintering of a 3D feeder screw pressed on a helical mandrel was investigated. A slightly inhomogeneous green density distribution is predicted after compaction. The residual stresses remaining after pressure release were also determined. The spring back of the part leads to contact pressures, which may be of the order of the green strength and hence may cause problems in removing the part from the helical core. To study the distortion during sintering, a physical model for solid state sintering was applied. It was found that the warpage due to green density gradients is only small.

## Acknowledgements

We gratefully acknowledge financial support of the Bayerische Forschungsstiftung (Project II-1/FORK-ERAM).

## References

[1] O. Coube, H. Riedel, Numerical simulation of metal powder die compaction with special consideration of cracking, Powder Metall. 43 (2000) 123–131.
[2] PM Modnet Computer Modelling Group, Comparison of computer models representing powder compaction process—state of the art review, Powder Metall. 42 (1999) 301–311.
[3] A.C.F. Cocks, Constitutive modelling of powder compaction and sintering, Prog. Mater. Sci. 46 (2001) 201–229.
[4] A. Lawley, L. Smith, J.E. Smugersky (Eds.), Proceedings of the Int. Conference on Process Modelling in Powder Metallurgy & Particulate Materials, MPIF, Princeton, 2002.
[5] R.J. Henderson, H.W. Chendler, A.R. Akisanya, H. Barber, B. Moriaty, Finite element modelling of cold isostatic pressing, J. Europ. Ceram. Soc. 20 (2000) 1121–1128.
[6] S. Shima, K. Mimura, Densification behaviour of ceramic powder, Int. J. Mech. Sci. 28 (1986) 53–59.
[7] H. Park, K.T. Kim, Consolidation behaviour of SiC powder under cold compaction, Mater. Sci. Eng. A299 (2001) 116–124.
[8] I.S. Sandler, F.L. DiMaggio, G.Y. Baladi, Generalized cap model for geological materials, J. Geotech. Eng. Div. ASCE 102 (1976) 683–699.
[9] D.C. Drucker, W. Prager, Appl. Math. 10 (1952) 157–175.
[10] R. Hibbitt, D. Karlsson, C. Sorensen, ABAQUS/Explicit® Users Manual, version 6.3, Pawtucket, RI, 2003.
[11] H.J. Song, H.W. Chandler, The determination of some properties of ceramic powders using a simple cylindrical apparatus, Br. Ceram. Trans. J. 89 (1990) 49–52.
[12] S. Strijbos, Friction between a powder compact and a metal wall, Sci. Ceram. 8 (1976) 415–427.
[13] H.G. Kim, J.W. Lee, K.T. Kim, The effect of a rubber mold on densification and deformation of a metal powder compact during cold isostatic pressing, Mater. Sci. Eng. A318 (2001) 174–182.
[14] T. Kraft, H. Riedel, Numerical simulation of die compaction and sintering, Powder Metall. 45 (2002) 227–231.
[15] T. Kraft, H. Riedel, Numerical simulation of solid state sintering—model and application, J. Europ. Ceram. Soc. (in press) [doi: 10.1016/S0955-2219(03)00222-X].